PRECISE MEAN ORBITAL ELEMENTS DETERMINATION FOR LEO MONITORING AND MAINTENANCE

Sofya Spiridonova[(1)], **Michael Kirschner**[(2)], **and Urs Hugentobler**[(3)]
[(1)]*DLR / GSOC, Münchener Str. 20, 82234 Weßling, Germany, , Tel. +49(8153)28-3492, sofya.spiridonova@dlr.de*
[(2)]*DLR / GSOC, Münchener Str. 20, 82234 Weßling, Germany, , Tel. +49(8153)28-1385, michael.kirschner@dlr.de*
[(3)]*Technische Universität München (TUM), Arcisstraße 21, 80333 Munich, Germany, , Tel. +49(89)289-231-95, urs.hugentobler@bv.tum.de*

Abstract: *Mean orbital elements can be used for monitoring the satellite's long-term behavior and for maneuver planning. In this paper, an analytical algorithm for conversion of osculating orbital elements into mean orbital elements is introduced and evaluated on several satellite missions. The accuracy of the mean orbital elements is estimated and the applications of the algorithm for determination of the relative satellite's motion are discussed.*

Keywords: *Mean Orbital Elements, Orbital Perturbations, Analytical Orbital Theories.*

1. Introduction

New satellite applications and concepts in satellite mission design pose challenging requirements for the accuracy of orbit determination and maintenance. In particular, data collection of satellite formations like GRACE 1 & 2 or TerraSAR-X and TanDEM-X introduces strict formation keeping requirements. For formation monitoring and maintenance as well as for orbit monitoring of single satellites, so-called *mean orbital elements* are often used. These elements are free from short-period perturbations and reveal the long-term behavior of the satellite's orbit. The mean orbital elements can be also used for maneuver planning and calculation. The straightforward computation of Δv from the required change in the semi-major axis Δa is the most direct approach to altitude corrections for satellites in circular orbits. For instance, in the case of the GRACE satellites, the required change in the mean semi-major axis of the maneuvering satellite is normally about 15-30 meters. Considering an acceptable error margin of 3% this leads to the requirement that Δa of the two satellites has to be resolved better than to 1 meter.

The topic of mean orbital elements has already been discussed many times in literature. Among the older publications are the papers [10] and [11], where two iterative procedures are described for the determination of the mean elements for the famous Brouwer's analytical theory, [4]. The newer publications on the topic include [5] and [13]. As the older analytical theories often do not deliver the required accuracy, and the implementation of the newer theories requires access to the internal documentation of other space agencies or journal papers of limited access, other available theories have been investigated to be implemented and operationally used at GSOC.

The method proposed in this paper is a combination of theories developed by Eckstein, Ustinov and Kaula ([1], [2] and [3]), and will be further referred to as EUK. It allows to calculate analytically first order perturbations due to arbitrary degree and order, as well as second-order perturbations

due to the oblateness term J_2. The remaining higher-order variations in the mean semi-major axis are restricted to ± 1.5 meters. Thus, the required accuracy is achieved analytically, with no time-expenses of numerical averaging and no problems of inaccurate orbit sampling. Further numerical averaging over one orbit proves to be sufficient to achieve a sub-meter accuracy in the determination of the mean semi-major axis. In the case of satellites in a formation (e.g. GRACE), their Δa, required for the planning of the station-keeping cycles, can be calculated to the accuracy of a few centimeters.

Section 2. contains an overview of the applied perturbation theories and describes the suggested algorithm. Some results of the algorithm evaluated on TOPEX/Poseidon, GRACE and TerraSAR-X propagated orbital elements are presented in section 3. Section 4. demonstrates the performance of the algorithm in the determination of Δa of the GRACE satellites at the end of several station-keeping cycles as well as gives an insight into the typical errors of the algorithm applied to maneuver post-processing. Finally, section 5. provides a summary of the accomplished work.

2. Theoretical background

2.1. Kaula's theory

Kaula's linear perturbation theory (LPT), developed in [1], has been applied since 1966 in many geodetic areas, e.g. ground-tracking of the satellites, altimetry, SST, and space-borne gravity gradiometry. It is based on the well-known Lagrange planetary equations

$$\begin{aligned}
\frac{da}{dt} &= \frac{2}{na}\frac{\partial R}{\partial M} \\
\frac{de}{dt} &= \frac{1-e^2}{na^2e}\frac{\partial R}{\partial M} - \frac{\sqrt{1-e^2}}{na^2e}\frac{\partial R}{\partial \omega} \\
\frac{di}{dt} &= \frac{\cos i}{na^2\sqrt{1-e^2}\sin i}\frac{\partial R}{\partial \omega} - \frac{1}{na^2\sqrt{1-e^2}\sin i}\frac{\partial R}{\partial \Omega} \\
\frac{d\Omega}{dt} &= \frac{1}{na^2\sqrt{1-e^2}\sin i}\frac{\partial R}{\partial i} \\
\frac{d\omega}{dt} &= \frac{\sqrt{1-e^2}}{na^2e}\frac{\partial R}{\partial e} - \frac{\cos i}{na^2\sqrt{1-e^2}\sin i}\frac{\partial R}{\partial i} \\
\frac{dM}{dt} &= n - \frac{1-e^2}{na^2e}\frac{\partial R}{\partial e} - \frac{2}{na}\frac{\partial R}{\partial a},
\end{aligned}$$

which describe the satellite's motion in terms of its Keplerian elements a, e, i, Ω, ω, M, and the so-called perturbing potential R.

Without going into the details of derivation, the perturbing potential R can be represented as a function of Keplerian orbital elements

$$R = \sum_{l=2}^{L} \frac{\mu a_e^l}{a^{l+1}} \sum_{m=0}^{l} \sum_{p=0}^{l} F_{lmp}(i) \sum_{q=-\infty}^{q=+\infty} G_{lpq}(e) S_{lmpq}(\omega, M, \Omega, \theta),$$

where a_e is the Earth's equatorial radius, θ is Greenwich sidereal time, $F_{lmp}(i)$ and $G_{lpq}(e)$ are the inclination and eccentricity functions. Here

$$S_{lmpq} = \begin{cases} C_{lm}\cos\psi_{lmpq} + S_{lm}\sin\psi_{lmpq}, & \text{if } l-m \text{ is even,} \\ -S_{lm}\cos\psi_{lmpq} + C_{lm}\sin\psi_{lmpq}, & \text{if } l-m \text{ is odd,} \end{cases} \tag{1}$$

and

$$\psi_{lmpq} = (l-2p)\omega + (l-2p+q)M + m(\Omega-\theta). \tag{2}$$

The exact formulas for the inclination functions F_{lmp} and the eccentricity functions G_{lpq} can be found in [1].

As we can see from (1), every elementary potential R_{lmpq} is a harmonic function of ψ_{lmpq}. Several different cases can be considered depending on the period of ψ_{lmpq}. Elementary potentials R_{lmpq} with $l-2p+q \neq 0$ have frequencies that are multiples of the satellite revolution frequency. Corresponding orbit variations are referred to as short-period perturbations. Another type of perturbations is caused by R_{lmpq} with $l-2p+q=0$ and $m \neq 0$. They have frequencies that are multiples of the Earth revolution frequency, and a period equal to or shorter than the Earth's rotation period, therefore, such perturbations are referred to as medium-period or m-daily perturbations. Elementary potentials R_{lmpq} with $l-2p+q=0$, $m=0$, and $l-2p \neq 0$ lead to long-period perturbations, whereas terms where all coefficients in (2) are zero, cause secular variations.

The integration of the Lagrange equations under the assumption that the time dependency on the right side comes only from the secular rates of the angular elements, delivers the following expressions for perturbations:

$$\begin{aligned}
\Delta a_{lmpq} &= \frac{\mu a_e^l}{n_0 a_0^{l+2}} 2F_{lmp}G_{lpq}(l-2p+q)\frac{S_{lmpq}}{\dot{\psi}_{lmpq}} \\
\Delta e_{lmpq} &= \frac{\mu a_e^l}{n_0 a_0^{l+3} e_0} F_{lmp}G_{lpq}\left[\sqrt{1-e_0^2}(l-2p+q) - (l-2p)\right]\frac{S_{lmpq}}{\dot{\psi}_{lmpq}} \\
\Delta i_{lmpq} &= \frac{\mu a_e^l}{n_0 a_0^{l+3}\sqrt{1-e_0^2}\sin i_0} F_{lmp}G_{lpq}\left[(l-2p)\cos i_0 - m\right]\frac{S_{lmpq}}{\dot{\psi}_{lmpq}} \\
\Delta\Omega_{lmpq} &= \frac{\mu a_e^l}{n_0 a_0^{l+3}\sqrt{1-e_0^2}\sin i_0}\frac{\partial F_{lmp}}{\partial i}G_{lpq}\frac{\widetilde{S}_{lmpq}}{\dot{\psi}_{lmpq}} \\
\Delta\omega_{lmpq} &= \frac{\mu a_e^l}{n_0 a_0^{l+3}}\left[\frac{\sqrt{1-e_0^2}}{e_0}F_{lmp}\frac{\partial G_{lpq}}{\partial e} - \frac{\cot i_0}{\sqrt{1-e_0^2}}\frac{\partial F_{lmp}}{\partial i}G_{lpq}\right]\frac{\widetilde{S}_{lmpq}}{\dot{\psi}_{lmpq}} \\
\Delta M_{lmpq} &= \frac{\mu a_e^l}{n_0 a_0^{l+3}}\left[-\frac{\sqrt{1-e_0^2}}{e_0}\frac{\partial G_{lpq}}{\partial e} + 2(l+1)G_{lpq}\right]F_{lmp}\frac{\widetilde{S}_{lmpq}}{\dot{\psi}_{lmpq}},
\end{aligned}$$

where all the functions on the right-hand side are evaluated on the mean precessing ellipse. All the used notations and derivations of the formulas can be found in [1].

2.2. Eckstein-Ustinov's theory

The Eckstein-Ustinov's analytical satellite theory was first developed by Ustinov in [3] and later corrected by Eckstein in [2]. The advantage of the theory is that instead of the usual Keplerian elements it employs non-singular elements a, h, l, i, Ω, λ, where

$$\begin{aligned} h &= e\sin\omega \\ l &= e\cos\omega \\ \lambda &= \omega + M. \end{aligned}$$

The Lagrange equations expressed in terms of these elements are

$$\begin{aligned}
\frac{da}{dt} &= \frac{2}{na}\frac{\partial R}{\partial \lambda}, \\
\frac{dh}{dt} &= \frac{\sqrt{1-h^2-l^2}}{na^2}\left[\frac{\partial R}{\partial l} - \frac{h}{1+\sqrt{1-h^2-l^2}}\frac{\partial R}{\partial \lambda}\right] \\
&\quad - \frac{l\cot i}{na^2\sqrt{1-h^2-l^2}}\frac{\partial R}{\partial i} \\
\frac{dl}{dt} &= \frac{\sqrt{1-h^2-l^2}}{na^2}\left[\frac{\partial R}{\partial h} + \frac{l}{1+\sqrt{1-h^2-l^2}}\frac{\partial R}{\partial \lambda}\right] \\
&\quad - \frac{h\cot i}{na^2\sqrt{1-h^2-l^2}}\frac{\partial R}{\partial i} \\
\frac{di}{dt} &= \frac{\cot i}{na^2\sqrt{1-h^2-l^2}}\left(l\frac{\partial R}{\partial h} - h\frac{\partial R}{\partial l} + \frac{\partial R}{\partial \lambda}\right) - \frac{\csc i}{na^2\sqrt{1-h^2-l^2}}\frac{\partial R}{\partial \Omega} \\
\frac{d\Omega}{dt} &= \frac{\csc i}{na^2\sqrt{1-h^2-l^2}}\frac{\partial R}{\partial i} \\
\frac{d\lambda}{dt} &= n - \frac{2}{na}\frac{\partial R}{\partial a} + \frac{\sqrt{1-h^2-l^2}}{1+\sqrt{1-h^2-l^2}}\frac{1}{na^2}\left(h\frac{\partial R}{\partial h} + l\frac{\partial R}{\partial l}\right) \\
&\quad - \frac{\cot i}{na^2\sqrt{1-h^2-l^2}}\frac{\partial R}{\partial i}.
\end{aligned} \tag{3}$$

We can observe that the eccentricity has disappeared from the denominators, and thus the Eckstein-Ustinov's theory, as opposed to Kaula's, is valid for zero eccentricity.

Another advantage of the Ekstein-Ustinov's theory is that it is among the very few theories where not only long-periodic, but also short-periodic perturbations in the semi-major axis are developed to the second order. Removing second-order short-periodic perturbations from the osculating semi-major axis is essential for meeting our accuracy requirements, but is often neglected by propagator-type theories, where secular and long-period perturbations affecting long-term behavior of the elements are considered of greater interest.

In the development of Ustinov's theory, the eccentricity is assumed to be of order J_2. Zonal harmonics are considered up to C_{60}, and tesseral harmonics up to degree and order 4. As in Kaula,

the elements on the right-hand side of the transformed Lagrange equations (3) are considered to be constant in the first iteration of the integration. In the second iteration, the first-order solution is substituted on the right-hand side of (3) and integrated to obtain the second-order solution. The theory was formulated by Ustinov as an analytical propagator, where initial mean elements are estimated iteratively, and then secular, long-, medium-, and short-periodic perturbations are calculated as functions of the initial mean elements and added to the initial mean elements to obtain the osculating elements at epoch.

For our purposes, only J_2 perturbations of first and second order were kept. However, this second-order J_2-solution is not fully consistent, because J_2^2-terms were neglected everywhere except for in the semi-major axis. These terms are, however, still smaller than other second-order terms hJ_2 and lJ_2, [2]. The following expressions for the J_2-induced short-periodic perturbations are the simplified ones from [2].

$$\begin{aligned}
\Delta a &= -\frac{3a_0}{2\lambda'}G_{20}\left[\left(2-\frac{7}{2}\beta_0^2\right)l_0\cos\lambda_0+\left(2-\frac{5}{2}\beta_0^2\right)h_0\sin\lambda_0\right.\\
&\quad\left.+\beta_0^2\cos 2\lambda_0+\frac{7}{2}\beta_0^2(l_0\cos 3\lambda_0+h_0\sin 3\lambda_0)\right]\\
&\quad+\frac{3a_0}{4}G_{20}^2\beta_0^2\left[7(2-3\beta_0^2)\cos 2\lambda_0+\beta_0^2\cos 4\lambda_0\right]\\
\Delta h &= -\frac{3}{2\lambda'}G_{20}\left[\left(1-\frac{7}{4}\beta_0^2\right)\sin\lambda_0+(1-3\beta_0^2)l_0\sin 2\lambda_0\right.\\
&\quad\left.+\left(-\frac{3}{2}+2\beta_0^2\right)h_0\cos 2\lambda_0+\frac{7}{12}\beta_0^2\sin 3\lambda_0+\frac{17}{8}\beta_0^2(l_0\sin 4\lambda_0-h_0\cos 4\lambda_0)\right]\\
\Delta l &= -\frac{3}{2\lambda'}G_{20}\left[\left(1-\frac{5}{4}\beta_0^2\right)\cos\lambda_0+\frac{1}{2}(3-5\beta_0^2)l_0\cos 2\lambda_0\right.\\
&\quad\left.+\left(2-\frac{3}{2}\beta_0^2\right)h_0\sin 2\lambda_0+\frac{7}{12}\beta_0^2\cos 3\lambda_0+\frac{17}{8}\beta_0^2(l_0\cos 4\lambda_0+h_0\sin 4\lambda_0)\right]\\
\Delta i &= -\frac{3}{4\lambda'}G_{20}\beta_0\sqrt{1-\beta_0^2}\left[-l_0\cos\lambda_0+h_0\sin\lambda_0\right.\\
&\quad\left.+\cos 2\lambda_0+\frac{7}{3}(l_0\cos 3\lambda_0+h_0\sin 3\lambda_0)\right]\\
\Delta\Omega &= \frac{3}{2\lambda'}G_{20}\sqrt{1-\beta_0^2}\left[\frac{7}{2}l_0\sin\lambda_0-\frac{5}{2}h_0\cos\lambda_0-\frac{1}{2}\sin 2\lambda_0\right.\\
&\quad\left.-\frac{7}{6}l_0\sin 3\lambda_0+\frac{7}{6}h_0\cos 3\lambda_0\right]
\end{aligned}$$

$$\Delta\lambda = -\frac{3}{2\lambda'}G_{20}\left[\left(10-\frac{119}{8}\beta_0^2\right)l_0\sin\lambda_0+\left(\frac{85}{8}\beta_0^2-9\right)h_0\cos\lambda_0\right.$$
$$+\left(2\beta_0^2-\frac{1}{2}\right)\sin 2\lambda_0+\left(-\frac{7}{6}+\frac{119}{24}\beta_0^2\right)(l_0\sin 3\lambda_0-h_0\cos 3\lambda_0)$$
$$-\left(3-\frac{21}{4}\beta_0^2\right)l_0\sin\lambda_0+\left(3-\frac{15}{4}\beta_0^2\right)h_0\cos\lambda_0$$
$$\left.-\frac{3}{4}\beta_0^2\sin 2\lambda_0-\frac{21}{12}\beta_0^2(l_0\sin 3\lambda_0-h_0\cos 3\lambda_0)\right],$$

where

$$\lambda' = 1-\frac{3}{2}G_{20}(3-4\beta_0), \quad \beta_0 = \sin i_0,$$

$$G_{20} = -J_2\left(\frac{a_e}{a}\right)^2, \quad a_e \text{ is the Earth's equatorial radius.}$$

The elements with zero-subscripts on the right-hand side of these formulas are J_2-mean elements at epoch and have to be determined iteratively.

2.3. Algorithm implementation

In the previous sections, the mathematical description of both theories used in the suggested algorithm was given. The practical realization, however, requires consideration of a few implementational aspects. First, these theories can not be applied straightforwardly, as both require mean elements for the computation of the perturbations. As we are dealing with the inverse problem, the perturbations have to be computed iteratively using the osculating elements, and then subtracted from them to obtain the mean elements. Second, neither of the two theories applied independently can deliver the required accuracy. Using the described modification of the Eckstein-Ustinov theory alone, the uncertainty in the semi-major axis reaches hundreds of meters, while applying Kaula's theory only, where no second-order J_2-perturbations are considered, leaves a variation of 7-30 meters in the mean semi-major axis, depending on the altitude. Therefore, a combination of the two theories is necessary.

The proposed approach can be divided into two main steps. The first step is an iterative calculation of the J_2-induced first- and second-order perturbations and the extraction of the J_2-mean elements with Eckstein-Ustinov theory. In the beginning of the first iteration, the mean elements are equal to the osculating elements. The output of each iteration is the set of the osculating elements obtained by adding the perturbations to the mean orbital elements. The result is transformed into a position-velocity vector and compared to the position-velocity vector obtained from the initial osculating elements. The difference between them is applied as a correction to the current position-velocity vector, which is transformed back to the set of the mean orbital elements. This process continues until the calculated position-velocity vector matches with the initial position-velocity vector to a predefined accuracy. The second step of the suggested algorithm is the calculation of the first-order

perturbations due to all other spherical harmonics with Kaula's theory and their subtraction from the J_2-mean elements obtained on the first step.

3. Evaluation and results

In this section, we shall compare the results of our algorithm with those presented in [5] by J.R. Guinn. In [5], a comparable algorithm for generating mean elements is presented and evaluated on propagated osculating elements of TOPEX/Poseidon. The difference to our approach is that in [5] the J_2-effects are calculated using a different theory of A. Konopliv, presented in [8]. In his simulations, J.R. Guinn considered the gravity field up to degree and order 17, and the effects of the Sun and the Moon. However, the air drag was not taken into account during the propagation. For the generation of mean elements, all harmonics up to degree and order 17 were considered.

Making use of the more precise information available today on gravity field we apply a force model, which includes a gravity field up to degree and order 60, as well as third-body effects from Sun and Moon. As in [5], no air drag was considered during propagation. Still, to facilitate the comparison with the results from [5], we remove the effects only up to degree and order 17. In the following, the resulting mean elements will be shown and discussed, with the exception of Ω and M, which we consider of minor interest due to their secular nature. All the plots corresponding to these two elements can be found in [14].

Semimajor axis. In Fig. 1 we can observe the osculating semi-major axis (black), dominated by

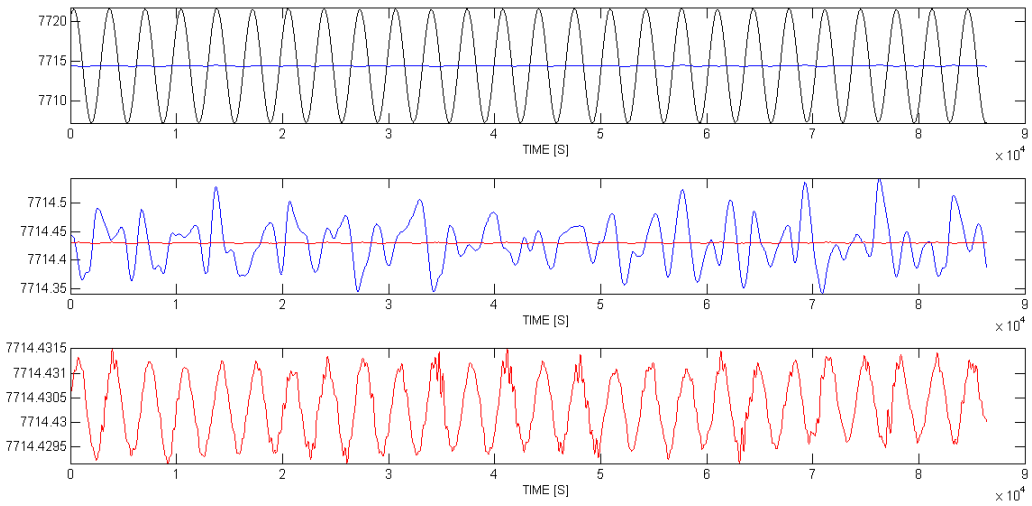

Figure 1. Semi-major axis, T/P, [km]: osculating (black), J_2-mean (blue), EUK (red)

the J_2-oscillations of about 15 kilometers in total, and J_2-mean semi-major axis (blue), which has a variation of 200 meters in total. In the lowest subplot, we can see the mean semi-major axis obtained with EUK (red), with a variation of ± 1.2 meters.

Eccentricity. In Fig. 2 we can see the osculating and mean eccentricities. After removing J_2-

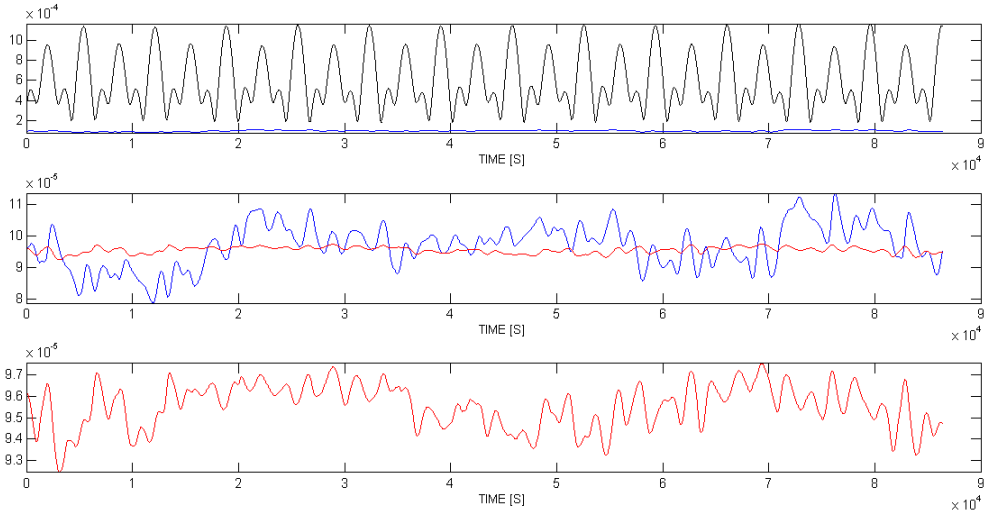

Figure 2. Eccentricity, T/P, [-]: osculating (black), J_2-mean (blue), EUK (red)

effects, the eccentricity drops to 9.5×10^{-5}, the target value of the frozen orbit of TOPEX/Poseidon, described in detail in [9]. Frozen orbits eliminate altitude variability over the same point on ground, being therefore advantageous for altimetry satellites. After removing the aspherical terms past J_2, the remaining variation in the mean eccentricity is of the order of $\pm 2.5 \times 10^{-6}$.

Inclination. As described in [9], the reference inclination of TOPEX/Poseidon is 66.0408 degrees,

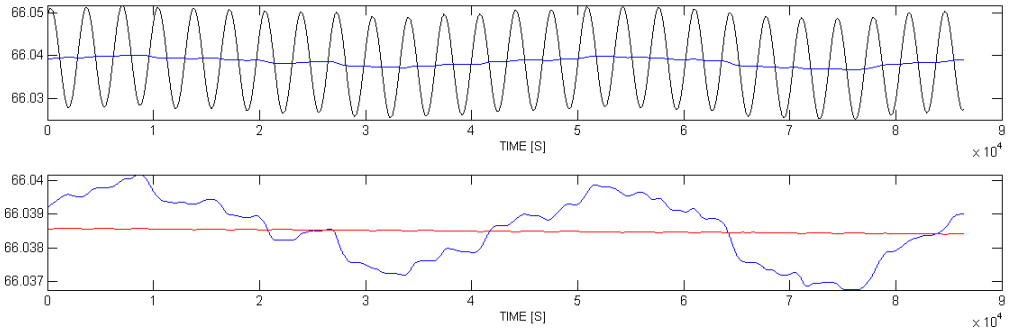

Figure 3. Inclination, T/P, [deg]: osculating (black), J_2-mean (blue), EUK (red)

selected to define the 10-days repeat-cycle. It is also close to the critical inclination of 63.4 degrees, which sets the J_2 contribution to secular variation in the argument of perigee to zero. In Fig. 3 we can see the osculating and mean inclination of TOPEX/Poseidon derived with EUK. Apart from the twice-per-revolution effect of J_2, the next dominating perturbation, clearly visible in the J_2-mean inclination (blue), is the twice-per-day variation due to the sectoral harmonics of degree and order 2. Removing it together with other aspherical terms leaves an almost linear trend with a slight decline.

Argument of perigee. In Fig. 4 we can see the osculating and mean arguments of perigee. Here

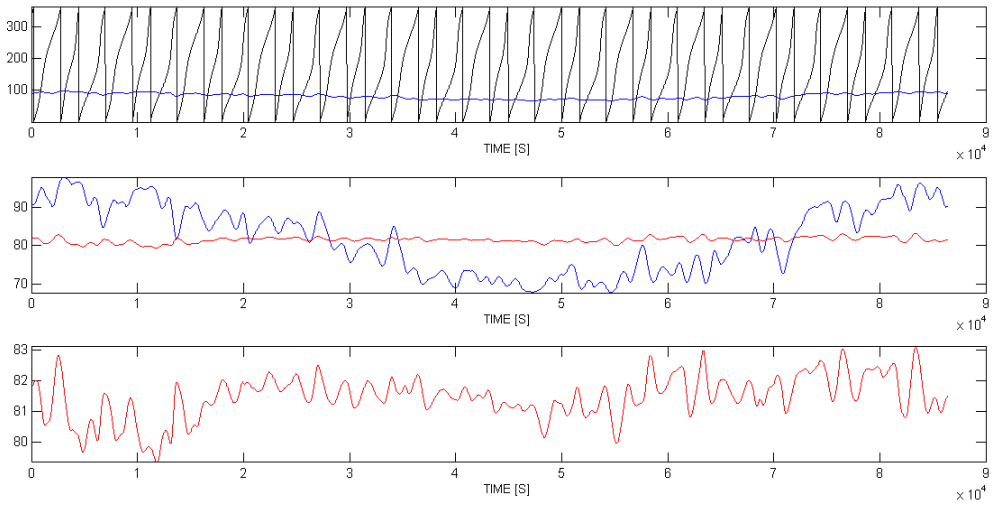

Figure 4. Argument of perigee, T/P, [deg]: osculating (black), J_2-mean (blue), EUK (red)

the mean value is approximately 81.3 degrees, and the remaining variation is about ± 2 degrees.

3.1. Comparison results

Table 1 summarizes the accuracies of the mean elements achieved with EUK for TOPEX/Poseidon, GRACE and TerraSAR-X propagated ephemeris. For the purpose of comparison, the 3rd column provides information on the accuracies achieved in [5]. The values were extracted from the graphs by visual inspection. The value marked with an asterisk refer to the variation of the element on top of the secular trend due to J_2. It should be noted that the accuracy of the mean elements in the context of this paper refers to the variation of the mean elements retrieved from the propagated osculating elements along a period of one day with no maneuvers. The inclination was omitted from the comparison, since in [5] it is plotted as in Fig. 3 against the J_2-mean inclination only, which makes a visual estimation of the variation impossible.

The conclusions we can draw from Tab. 1 is the similarity of the variation in a_{mean} obtained with the EUK algorithm, to the variations obtained in [5], and a better performance of EUK in e and ω, where the variations are both by factor 4 lower than those presented in [5]. However, it should be mentioned here, that the comparison with the results of [5] is complicated by the fact, that in [5] the sampling interval is 15 minutes, while in our case it is only 10 seconds. Therefore, the graphs from [5] are much coarser then ours.

4. Applications to the GRACE formation

Launched in March 2002, the GRACE formation was the first mission to explore formation flying for accurate retrieval of the Earth gravity field. Accurate pointing of the K-band antenna, the key

Table 1. Typical variations of the mean elements along one day.

OE	units	T/P ([5])	T/P (EUK)	GR 2 (EUK)	TS-X (EUK)
a_{mean}	[m]	~± 1.0	± 1.2	± 1.5	± 1.3
e_{mean}	[-]	~$\pm 1 \times 10^{-5}$	$\pm 2.5 \times 10^{-6}$	$\pm 4 \times 10^{-6}$	$\pm 6 \times 10^{-6}$
ω_{mean}	[deg]	~± 7.5	± 2.0	$\pm 0.08^{*}$	± 0.1

instrument for the mission objectives, requires a certain difference in attitude of the twin satellites. The associated difference in ballistic coefficients and the subsequent higher air drag exerted on the leading satellite leads to a faster decay of the leading satellite's altitude, as compared to the trailing satellite. The along-track separation of the two satellites as a function of the difference in their mean semi-major axis follows a perturbed parabolic profile. During a station keeping cycle, the difference in mean semi-major axes between the leading and the trailing satellite grows from about -15 to about +15 meters, while the relative separation increases from 170 to about 270 meters, reaching its maximum when the semi-major axes become equal, and then decreases again. An example of such cycle is given in Fig. 5. More details on the relative motion of the GRACE satellites are given in [6]

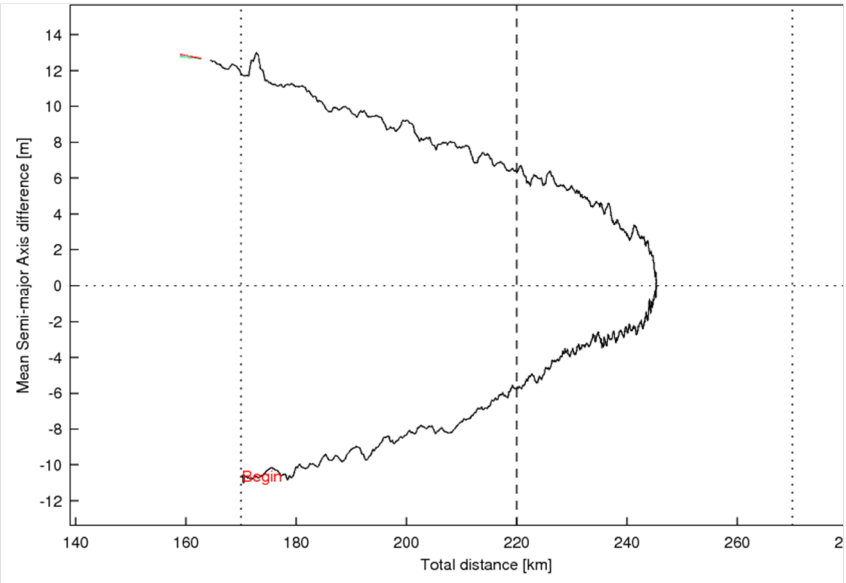

Figure 5. GRACE relative motion, prediction after the 18th orbit maintenance maneuver, initial epoch: 2011/08/17, nominal end epoch: 2012/03/01

and [7]. To maintain the along-track separation of the GRACE satellites in the required window between 170 and 270 meters, altitude maneuvers have to be performed every 6-12 months. In the meantime, Δa has to be properly monitored and at the end of the cycle accurately estimated for the transition to the next station keeping cycle. Figure 6 refers to the cycle which ended on July 4, 2012, with a maneuver of GRACE 2. Here we can see the mean semi-major axes of both GRACE satellites calculated with the suggested algorithm using their propagated osculating elements. The initial osculating elements were obtained with orbit determination a few days before the maneuver. No air drag was included in the propagator. The graphs show that the mean semi-major axes of GRACE 1 and GRACE 2 are at 6822.3796 kilometers and 6822.3867 kilometers respectively, both having the uncertainty of ± 1.9 meters. Taking the difference between the mean semi-major axes of

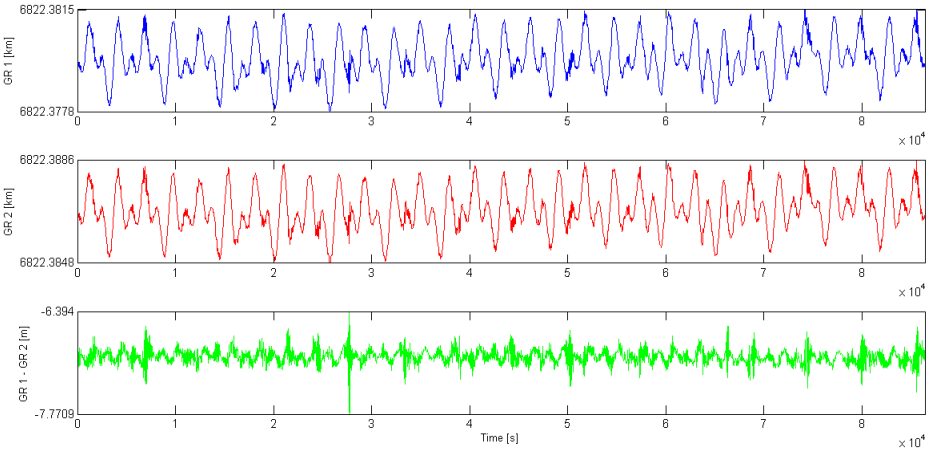

Figure 6. End of the 19th SK cycle, July 1, 2012: mean semi-major axes and Δa

the GRACE satellites, we obtain the green curve from the bottom subplot in Fig. 6. The mean value of Δa is about -7.08 meters with the variation of ± 0.68 meters.

To increase the accuracy of the estimated Δa, we can apply a further numerical averaging to the mean semi-major axes, obtained analytically with our algorithm. In Fig. 7 we can observe that the uncertainty of the mean semi-major axes of the GRACE satellites reduces to ± 0.25 meters after numerical averaging over one orbit, while the uncertainty in the corresponding Δa drops to ± 2.5 cm only. In a similar way, the mean semi-major axes of the two satellites and the corresponding Δa were

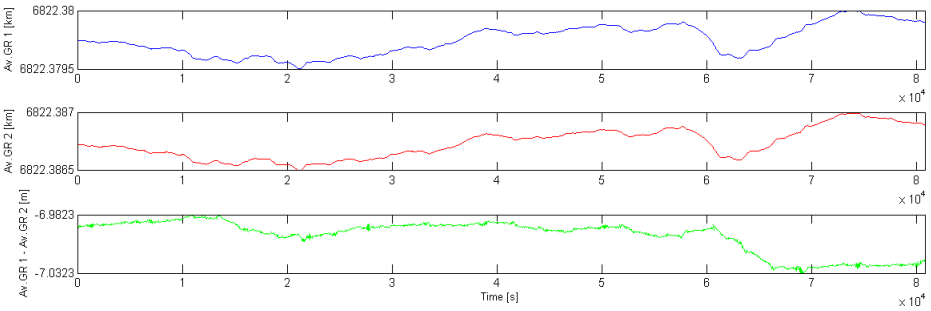

Figure 7. End of the 19th SK cycle, July 1, 2012: averaged mean semi-major axes and $\Delta \bar{a}$

estimated at the ends of some other station-keeping cycles. The accuracies of the estimation are summarized in Tab. 2. Again, it should be kept in mind that the accuracy in this context refers to the variation of the estimate along one day. The process currently employed at GSOC for calculation of the Δv required at the end of a station-keeping cycle starts at least one week in advance. Every day, the updated ephemeris (6 or 12 a.m.) are propagated using the most recent solar flux predictions until the approximate time of the maneuver. The semi-major axes are estimated by removing the first-order J_2 perturbation with a method based on the Brouwer analytical theory, and a subsequent numerical averaging over one day. After that, Δa at the time of the maneuver is calculated. This

Table 2. Typical variations of Δa (EUK), and with an additional numerical averaging.

Cycle Number	**Date**	**Δa, [m]**	**$\Delta\bar{a}$, [m]**
19	01/07/12	$\pm$0.68	$\pm$0.03
18	25/02/12	$\pm$0.69	$\pm$0.02
17	14/08/11	$\pm$0.42	$\pm$0.02
16	05/02/11	$\pm$0.39	$\pm$0.01

Table 3. Estimated Δa_{before} (rows 2 to 6), estimated Δa_{after} (row 7).

Time	$a_{\text{GR 1}}$	$a_{\text{GR 2}}$	$\Delta a_{\text{before/after}}$
06/30, 06:00:00	6822,3459372546	6822,3530179945	0,00708073990
07/01, 06:00:00	6822,3359996653	6822,3431186943	0,00711902900
07/02, 06:00:00	6822,3309448860	6822,3380632464	0,00711836041
07/03, 06:00:00	6822,3223709698	6822,3295054254	0,00713445552
07/04, 06:00:00	6822,3143787003	6822,3218741735	0,00749547314
07/04, 12:00:00	6822,3095570668	6822,2998930177	-0,00966404909

procedure is repeated once a day, while Δa calculated day by day is being influenced by the errors in solar flux prediction and the errors of the propagator.

This procedure was simulated for one of the cycles using EUK and the results are presented in Tab. 3. The starting epoch used in the propagator is indicated in the 1st column, while the 2nd and the 3rd columns show the two mean semi-major axes (EUK) at the epoch of the maneuver (04/07/12, 7:03:21 a.m.) in kilometers. As we can see from the table, the absolute mean semi-major axis varies from one day to another by as much as 10 meters. This is the result of the changing solar flux predictions. As the errors corresponding to the two satellites flying in quasi equal conditions are almost the same, the resulting variation of the Δa is only about $\pm$20 centimeters along those several days. Altogether, the difference between the mean semi-major axis before the maneuver can be estimated as $\Delta a_{\text{before}} = 7.28 \pm 0.20$ meters, whereas the difference between the semi-major axes after the maneuver is estimated as $\Delta a_{\text{after}} = -9.66$ meters (see last row).

Comparing $\Delta a_{\text{man}}^{\text{EUK}} = \Delta a_{\text{after}} - \Delta a_{\text{before}}$ to

$$\Delta a_{\text{man}} = -\frac{\Delta v \cdot 2a}{v}. \tag{4}$$

calculated directly from the performed maneuver $\Delta v = -0.009582$ m/s, we come to the conclusion, that the relative error of our estimate $\Delta a_{\text{man}}^{\text{EUK}}$ is 0.53%. Table 4 summarizes the results obtained in the same way for some other maneuvers of GRACE. Additionally to the station-keeping maneuvers of GRACE, one simulated maneuver was used to access the errors in case of large Δv. The results of it are provided in the last row of Tab. 4. There we can see a very high Δv as compared to the Δv's of the GRACE station-keeping maneuvers, and the corresponding high change in the mean semi-major axis. As we can see from Tab. 4, the error of our estimate in the occurred Δa is everywhere less than 3%. In 5 cases out of 8, the error lies below 1%. Due to the linear relation between Δa and Δv in (4) we can conclude that the performed Δv can be estimated with EUK with the same accuracy (better than 3%).

Table 4. Typical errors of $\Delta a_{\mathbf{man}}^{\mathbf{EUK}}$ w.r.t. $\Delta a_{\mathbf{man}}$.

Sat.	Date	a[km]	Δv[m/s]	$\Delta a_{\mathrm{man}}^{\mathrm{EUK}}$[m]	Δa_{man}[m]	Error[%]
GRACE	04.07.12	6822,30	0,009582	17,16	17,07	-0,53
GRACE	28.02.12	6826,00	0,013839	25,47	24,74	-2,95
GRACE	17.08.11	6832,25	0,009639	17,19	17,26	0,40
GRACE	08.02.11	6834,95	0,009209	16,52	16,50	-0,12
GRACE	19.05.10	6836,71	0,007543	13.75	13,52	-1.70
GRACE	13.08.09	6839,13	0,007602	13,72	13,63	-0,66
GRACE	28.07.09	6838,11	0,007042	12,29	12,62	2,61
TSX	08.08.12	6883,86	0,200000	359,75	362,10	0,65

5. Conclusions

The presented paper deals with the generation of mean orbital elements on the basis of the provided osculating orbital elements. Numerical averaging has a number of uncertainties and disadvantages as compared to analytical algorithms. Therefore, the aim of this paper is to introduce an analytical algorithm, namely, a combination of Eckstein-Ustinov's and Kaula's analytical theories for the conversion of osculating orbital elements into mean orbital elements.

The suggested algorithm was applied to propagated ephemeris of TOPEX/Poseidon, GRACE and TerraSAR-X. It was observed, that the uncertainty in the mean semi-major axis obtained with our algorithm is comparable to that obtained for TOPEX/Poseidon in [5] with a similar algorithm. At the same time, the uncertainties in two other important parameters of the orbit, the eccentricity and the argument of perigee, are both by factor 4 lower than the uncertainties shown in [5].

Considering that in the determination of the relative position of the GRACE satellites, one often deals with the values in the range of a few meters, the related inaccuracies have to be accordingly eliminated. Numerical averaging over one orbit of the mean semi-major axes obtained with the suggested analytical algorithm proved to be sufficient to achieve a sub-meter accuracy in the determination of the mean semi-major axis, and the accuracy of a few centimeters in the determination of the Δa of two satellites flying in a formation (e.g. GRACE).

Finally, the algorithm was used in a simulation of a part of a maneuver planning procedure. The Δa of the GRACE satellites estimated days before the maneuver shows a sub-meter stability. At the same time, the total change in the mean semi-major axis of GRACE 2 due to the maneuver was estimated using the suggested algorithm with the accuracy better than 3% in all the test runs.

The introduced algorithm has a comparable performance as the algorithm from [5]. The performance improves drastically after an additional numerical averaging over one orbit, reducing the variation in the semi-major axis to a sub-meter level, and the variation in Δa to a few centimeters only.

6. References

[1] W.M. Kaula, *Theory of satellite geodesy*, Blaisdell Publ. Company, Waltham, MA., (1966).

[2] M.C. Eckstein, H. Hechler, *A reliable derivation of the perturbations due to any zonal and tesseral harmonics of the geopotential for nearly-circular satellite orbits*, ESOC, ESRO SR-13 (1970).

[3] B.A. Ustinov, *Motion of satellites along low-eccentricity orbits in a noncentral terrestrial gravitational field*, Cosmic research **5** (1967), p.159.

[4] D. Brouwer, *Solution of the problem of artificial satellite theory without drag*, Astronomical J. **64** (1966), p. 378

[5] J.R. Guinn, *Periodic gravitational perturbations for conversion between osculating and mean orbit elements*, AAS/AIAA Astrodynamics Specialist Conference 91-430 (1991).

[6] M. Kirschner, O. Montenbruck, S. Bettadpur, *Flight Dynamics Aspects of the GRACE Formation Flying*, Proc. of 2nd Workshop on Satellite Constellations and Formation Flying, Haifa, Israel (2001).

[7] M. Kirschner, *First results on the implementation of the GRACE formation*, 3rd International Workshop On Satellite Constellations and Formations, 24-26 Feb. 2003, Pisa (2003)

[8] A. Konopliv, *A third-order J2 solution with a transformed time*, JPL IOM 314.3-970 (internal document), 28 March 1991.

[9] R.B. Frauenholz, R.S. Bhat, B.E. Shapiro, R.K. Leavitt, *Analysis of the TOPEX/Poseidon operational orbit: Observed variations and why*, J. of Spacecraft and Rockets **35**:2 (1998), 212-224

[10] B. Cain, *Determination of mean elements for Brouwer's satellite theory*, Astronomical J. **64**:6 (1962), p. 391

[11] H. Walter, *Conversion of osculating orbital elements into mean orbital elements*, Astronomical J. **72**:8 (1967), p. 994

[12] G. Chebotarev, *Analytical and numerical methods of celestial mechanics*, Publishing House *Nauka* (1965).

[13] E. Wnuk, *Prediction of artificial satellite positions on the basis of the second order theory of motion*, Adv. Space Res. **30**:2 (2002), p. 321

[14] S. Spiridonova, *Conversion of Osculating Orbital Elements into Mean Orbital Elements for Orbit Monitoring and Precise Maneuver Planning*, Master's Thesis, TU München, 2012.